THE METHOD OF FUNDAMENTAL SOLUTIONS WITH DUAL RECIPROCITY FOR THIN PLATES ON WINKLER FOUNDATIONS WITH ARBITRARY LOADINGS

C. C. Tsai *

Department of Information Technology
Toko University
Chia-Yi County, Taiwan 61363, R.O.C.

ABSTRACT

This paper describes the combination of the method of fundamental solutions (MFS) and the dual reciprocity method (DRM) as a meshless numerical method to solve problems of thin plates resting on Winkler foundations under arbitrary loadings, where the DRM is based on the augmented polyharmonic splines constructed by splines and monomials. In the solution procedure, the arbitrary distributed loading is first approximated by the augmented polyharmonic splines (APS) and thus the desired particular solution can be represented by the corresponding analytical particular solutions of the APS. Thereafter, the complementary solution is solved formally by the MFS. In the mathematical derivations, the real coefficient operator in the governing equation is decomposed into two complex coefficient operators. In other words, the solutions obtained by the MFS-DRM are first treated in terms of these complex coefficient operators and then converted to real numbers in suitable ways. Furthermore, the boundary conditions of lateral displacement, slope, normal moment, and effective shear force are all given explicitly for the particular solutions of APS as well as the kernels of MFS. Finally, numerical experiments are carried out to validate these analytical formulas.

Keywords : Method of fundamental solutions, Dual reciprocity method, Kirchhoff plates, Winkler foundation.

1. INTRODUCTION

In the last decade, researchers have paid attention to the meshless numerical methods without employing the concept of elements. Some parts among these meshless numerical methods are based on the concept of representing the thought function by radial basis functions (RBFs). In 1990, Kansa [1] developed the multiquadrics (MQ) method that used the RBFs to approximate the governing equations and boundary conditions simultaneously. On the other hand, Kupradze and Aleksidze [2] discovered the method of fundamental solutions (MFS) by adopting the fundamental solutions as the RBFs and locating the sources of these fundamental solutions away from the computational domains. Recently, some researches also consider the possibility of locating the sources on the boundary [3-6]. Reviews of the MFS can be found in the recent literature [7,8]. Although the MFS has an advantage over the MQ method that it requires only boundary collocations, its usage is limited to homogeneous partial differential equations. Detailed descriptions and comparisons of the MQ method and the MFS can be found in [9]. Specially, the MFS performed better for eigenproblems [10,11].

In the applications of traditional boundary element method, a lot of computational effort is required to calculate the domain integration for the source term. The dual reciprocity method (DRM) was thus first introduced by Nardini and Brebbia [12] to transfer the domain integral to boundary type by a series of RBFs in their pioneer work. On the other hand, Golberg [13] first combined the MFS and the DRM as a meshless numerical method to solve Poisson's equation. Later, Golberg and Chen [14] extended the MFS-DRM to Helmholtz and diffusion problems. In these works, the nonhomogeneous source terms were approximated by augmented polynomial splines introduced by Duchon [15], which are constructed by splines and monomials. Thereafter, the MFS-DRM became a mature meshless numerical method to solve nonhomogeneous partial differential equations.

Although the MFS has been applied successfully to solve various partial differential equations, none of previous studies considered the MFS to problems that required kernels of complex coefficient operators. For problems of thin plates resting on Winkler foundations under arbitrary loadings, it involves the product opera-

* Assistant Professor

tor of two Helmholtz-type operators with complex coefficients. In this paper, we study the MFS to problems involving the product of two Helmholtz-type operators with complex coefficients based on the general theory mathematically established by Bogomolny [16]. On the other hand, the difference trick [17] is a well-known method to construct the fundamental solution for the product of some Helmholtz-type operators. In this work, we utilize the difference trick to find the analytical particular solutions of augmented polynomial splines for the product of two Helmholtz-type operators with complex coefficients. The analytical particular solutions for an individual Helmholtz-type operator are referred to the works of Cheng [18] and Golberg *et al*. [19] for splines and monomials respectively. It should be noted that the analytical particular solutions of monomials are also applicable when the Chebyshev method [20] is applied. Also, the explicit formula for the lateral displacement, slope, normal moment, and effective shear force are addressed for the kernels of MFS and the analytical particular solutions of DRM. Recently, the analytical particular solutions of multi-Helmholtz-type equation are alternatively derived [21].

A brief outline of the paper is as follows. We introduce the formulations of MFS-DRM for solving problems of thin plates resting on Winkler foundations under arbitrary loadings in Section 2. In Section 3, some numerical experiments are preformed and the issues of practically implementing the MFS-DRM are stated. Finally, the conclusions are summarized in Section 4.

2. MFS-DRM FORMULATION

Consider a thin plate resting on Winkler foundation in bending, with thickness h and midplane in the x_1-x_2 plane. According to the basic assumption of the Kirchhoff theory, the lateral deflection u is considered to be independent of x_3, and the transverse stressed are ignored. For homogeneous, isotropic, elastic plate, it is governed by [22,23]

$$(D\nabla^2\nabla^2 + k)\, u(\mathbf{x}) = q(\mathbf{x}) \quad \text{in} \quad \Omega \tag{1}$$

where is $q(\mathbf{x})$ is the density of lateral force at $\mathbf{x}$ = (x_1, x_2), k is the foundation stiffness, and $D = \dfrac{Eh^3}{12(1-v)}$ with E the Young's Modulus and v the Poisson's ratio of elasticity. For simplicity, we may let $\lambda^4 = \dfrac{k}{D}$ then Eq. (1) reduces to

$$D(\nabla^2\nabla^2 + \lambda^4)\, u(\mathbf{x}) = q(\mathbf{x}) \quad \text{in} \quad \Omega \tag{2}$$

Eq. (2) can also been rewritten as

$$D(\nabla^2 - \lambda_1^2)(\nabla^2 - \lambda_2^2)\, u(\mathbf{x}) = q(\mathbf{x}) \quad \text{in} \quad \Omega \tag{3}$$

with $\lambda_1 = \lambda e^{\mathbf{i}\frac{\pi}{4}}$ and $\lambda_2 = \lambda e^{-\mathbf{i}\frac{\pi}{4}}$. In other words, the real coefficient operator in the governing equation (Eq. (2)) can be decomposed into two complex coefficient operators in Eq. (3).

Furthermore, some proper boundary conditions should be imposed:

$$\begin{aligned} B_1 u(\mathbf{x}) &= \bar{u}_1(\mathbf{x}) \quad \text{on} \quad \Gamma \\ B_2 u(\mathbf{x}) &= \bar{u}_2(\mathbf{x}) \quad \text{on} \quad \Gamma \end{aligned} \tag{4}$$

where $\bar{u}_1(\mathbf{x})$ and $\bar{u}_2(\mathbf{x})$ are the given boundary data and the boundary operators B_1 and B_2 are any two of the following operators:

$$\mathbf{K}_u(\bullet) = 1 \tag{5a}$$

$$\mathbf{K}_\theta(\bullet) = \frac{\partial(\bullet)}{\partial \mathbf{n_x}} \tag{5b}$$

$$\mathbf{K}_m(\bullet) = \nu\, \nabla_\mathbf{x}^2(\bullet) + (1-\nu)\frac{\partial^2(\bullet)}{\partial \mathbf{n_x}^2} \tag{5c}$$

$$\mathbf{K}_v(\bullet) = \frac{\partial \nabla_\mathbf{x}^2(\bullet)}{\partial \mathbf{n_x}} + (1-\nu)\frac{\partial}{\partial \mathbf{t_x}}\frac{\partial^2(\bullet)}{\partial \mathbf{n_x}\partial \mathbf{t_x}} \tag{5d}$$

where $\dfrac{\partial}{\partial \mathbf{n_x}}$ and $\dfrac{\partial}{\partial \mathbf{t_x}}$ are the normal and tangential derivatives, respectively, on the boundary point $\mathbf{x}$. Eq. (5) can also be written in terms of the outward normal $\mathbf{n_x}$ = (n_1, n_2) as follows:

$$\mathbf{K}_u(\bullet) = 1 \tag{6a}$$

$$\mathbf{K}_\theta(\bullet) = \frac{\partial(\bullet)}{\partial x_1}n_1 + \frac{\partial(\bullet)}{\partial x_2}n_2 \tag{6b}$$

$$\mathbf{K}_m(\bullet) = \frac{\partial^2(\bullet)}{\partial x_1^2}\varepsilon_1 + \frac{\partial^2(\bullet)}{\partial x_1 \partial x_2}\varepsilon_2 + \frac{\partial^2(\bullet)}{\partial x_2^2}\varepsilon_3 \tag{6c}$$

$$\mathbf{K}_v(\bullet) = \frac{\partial^3(\bullet)}{\partial x_1^3}\kappa_1 + \frac{\partial^3(\bullet)}{\partial x_1^2 \partial x_2}\kappa_2 + \frac{\partial^3(\bullet)}{\partial x_1 \partial x_2^2}\kappa_3 + \frac{\partial^3(\bullet)}{\partial x_2^3}\kappa_4 \tag{6d}$$

with

$$\varepsilon_1 = Dn_1^2 + \nu\, Dn_2^2 \tag{7a}$$

$$\varepsilon_2 = 2(1-\nu)\, Dn_1 n_2 \tag{7b}$$

$$\varepsilon_3 = Dn_2^2 + \nu\, Dn_1^2 \tag{7c}$$

$$\kappa_1 = Dn_1(1+n_2^2) - \nu\, Dn_1 n_2^2 \tag{7d}$$

$$\kappa_2 = \nu\, Dn_2(1+n_1^2) + 2(1-\nu)Dn_2^3 - Dn_1^2 n_2 \tag{7e}$$

$$\kappa_3 = \nu\, Dn_1(1+n_2^2) + 2(1-\nu)Dn_1^3 - Dn_2^2 n_1 \tag{7f}$$

$$\kappa_4 = \nu\, Dn_2(1+n_1^2) - \nu\, Dn_2 n_1^2 \tag{7g}$$

In the above equations we denote $\mathbf{K}_u(u(\mathbf{x}))$, $\mathbf{K}_\theta(u(\mathbf{x}))$, $\mathbf{K}_m(u(\mathbf{x}))$, and $\mathbf{K}_v(u(\mathbf{x}))$ the lateral displacement, the slope, the normal moment, and the effective shear force respectively. Formally, (5a) and (5b) are selected for clamped boundary condition, (5a) and (5c) for simply-supported boundary condition, and (5c) and (5d) for free boundary condition.

In the MFS-DRM formulation, we linearly decompose the solution into

$$u(\mathbf{x}) = u_h(\mathbf{x}) + u_p(\mathbf{x}) \tag{8}$$

where the particular solution, $u_p(\mathbf{x})$, satisfies

$$D(\nabla^2\nabla^2 + \lambda^4)\, u_p(\mathbf{x}) = q(\mathbf{x}) \quad \text{in} \quad \Omega \tag{9}$$

and the homogenous solution, $u_h(\mathbf{x})$, satisfies

$$D(\nabla^2\nabla^2 + \lambda^4)\, u_h(\mathbf{x}) = 0 \quad \text{in} \quad \Omega \tag{10}$$

as well as the boundary conditions

$$\begin{aligned} B_1 u_h(\mathbf{x}) &= \bar{u}_1(\mathbf{x}) - B_1 u_p(\mathbf{x}) \quad \text{on} \quad \Gamma \\ B_2 u_h(\mathbf{x}) &= \bar{u}_2(\mathbf{x}) - B_2 u_p(\mathbf{x}) \quad \text{on} \quad \Gamma \end{aligned} \tag{11}$$

In the MFS-DRM formulation, the particular solution is first approximated by the DRM [13,14] and then the homogeneous problem can be solved by the MFS [16], whose details will be described in the following sections.

2.1 Dual Reciprocity Method

Now, we are in a position to introduce the DRM. When the augmented polyharmonic splines are adopted in the DRM, the force term $q(\mathbf{x})$ is approximated by

$$q(\mathbf{x}; \alpha^j, \beta^j) \cong \sum_{j=1}^{M} \alpha^j p^j(\mathbf{x}) + \sum_{j=1}^{N} \beta^j f(r_j) \tag{12}$$

where monomial basis consists of the family

$$\{p^1, p^2, \ldots, p^M\} = \{1, x_1, x_2, x_1^2, x_2^2, x_1 x_2, x_1^3, \ldots\} \tag{13}$$

and $f(r_j) = r_j^{2n} \ln r_j$ is the n-th order polyharmonic spline. In Eqs. (12) and (13), $r_j = \|\mathbf{x} - \mathbf{x}_j\|$ is the Euclidean distance between the coordinates $\mathbf{x}$ and the prescribed points $\mathbf{x}_j$ as depicted in Fig. 1.

Then, the $M + N$ unknown coefficients, α^j and β^j, can be determined by collocation and constraint conditions as follows

$$q(\mathbf{x}_i; \alpha^j, \beta^j) = \sum_{j=1}^{M} \alpha^j p^j(\mathbf{x}_i) + \sum_{j=1}^{N} \beta^j f(r_{ij}) \quad \text{for} \quad i = 1, 2, \ldots, N \tag{14a}$$

$$\sum_{j=1}^{N} \beta^j p^i(\mathbf{x}_j) = 0 \quad \text{for} \quad i = 1, 2, \ldots, M \tag{14b}$$

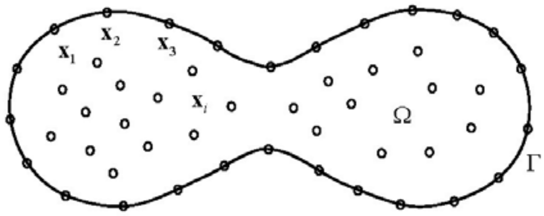

Fig. 1 Geometry configuration of the DRM

where $r_{ij} = \|\mathbf{x}_i - \mathbf{x}_j\|$. More details can be found in [15].

In the spirit of DRM, the particular solution $u_p(\mathbf{x})$ is assumed as follows:

$$u_p(\mathbf{x}) \cong \sum_{j=1}^{M} \alpha^j p^j(\mathbf{x}) + \sum_{j=1}^{N} \beta^j F(r_j) \tag{15}$$

in which $P^j(\mathbf{x})$, $F(r_j)$ are governed by

$$D(\nabla^2\nabla^2 + \lambda^4)\, P^j(\mathbf{x}) = p^j(\mathbf{x}) \tag{16a}$$

$$D(\nabla^2\nabla^2 + \lambda^4)\, F(r_j) = f(r_j) \tag{16b}$$

Details of $P^j(\mathbf{x})$ and $F(r_j)$ will be given in the later subsection. Then, the boundary conditions of the particular solutions can be obtained by using Eqs. (5) and (6) as follows:

$$B_1 u_p(\mathbf{x}) \cong \sum_{j=1}^{M} \alpha^j B_1 P^j(\mathbf{x}) + \sum_{j=1}^{N} \beta^j B_1 F(r_j) \tag{17a}$$

$$B_2 u_p(\mathbf{x}) \cong \sum_{j=1}^{M} \alpha^j B_2 P^j(\mathbf{x}) + \sum_{j=1}^{N} \beta^j B_2 F(r_j) \tag{17b}$$

To complete Eq. (17), the partial derivatives $\dfrac{\partial F(r)}{\partial x_i}$, $\dfrac{\partial^2 F(r)}{\partial x_i \partial x_j}$, $\dfrac{\partial^3 F(r)}{\partial x_i \partial x_j \partial x_k}$, $\dfrac{\partial P(\mathbf{x})}{\partial x_i}$, $\dfrac{\partial^2 P(\mathbf{x})}{\partial x_i \partial x_j}$, and $\dfrac{\partial^3 P(\mathbf{x})}{\partial x_i \partial x_j \partial x_k}$ should be supplied which are given in Appendix I.

2.2 Method of Fundamental Solutions

After the particular solution is solved, the homogeneous boundary value problem governed by Eqs. (10) and (11) becomes well defined. Thus, the homogeneous solution can be solved by the well-known MFS. In the spirit of the MFS, the homogeneous solution can be represented as [16]:

$$u_h(\mathbf{x}; \bar{\gamma}_1^j, \bar{\gamma}_2^j, \mathbf{s}_j) \cong \sum_{j=1}^{L} \bar{\gamma}_1^j \bar{G}_1(\mathbf{x}, \mathbf{s}_j) + \sum_{j=1}^{L} \bar{\gamma}_2^j \bar{G}_2(\mathbf{x}, \mathbf{s}_j) \tag{18}$$

where the kernels $\bar{G}_1(\mathbf{x}, \mathbf{s}_j) = K_0(\lambda_1 r_j)$ and $\bar{G}_2(\mathbf{x}, \mathbf{s}_j) = K_0(\lambda_2 r_j)$ are related to the fundamental solutions of $(\nabla^2 - \lambda_1^2)$ and $(\nabla^2 - \lambda_2^2)$ respectively as follows:

$$(\nabla^2 - \lambda_1^2)\, \bar{G}_1 = -2\pi\, \delta(\mathbf{x} - \mathbf{s}) \tag{19a}$$

$$(\nabla^2 - \lambda_2^2)\, \bar{G}_2 = -2\pi\, \delta(\mathbf{x} - \mathbf{s}) \tag{19b}$$

with $\delta(\mathbf{x}-\mathbf{s})$ the Dirac delta function and $r_j = \|\mathbf{x}-\mathbf{s}_j\|$. In Eq. (18), $K_0(\bullet)$ is the zero order modified Bessel function of second kind. Bogomolny [16] stated that solutions of Eq. (10) can be approximated arbitrarily close if L is sufficient large. Since the homogeneous solution u_h is a real function, it is wise to modify the Eq. (18) to

$$u_h(\mathbf{x};\gamma_1^j,\gamma_2^j,\mathbf{s}_j) \cong \sum_{j=1}^{L}\gamma_1^j G_1(\mathbf{x},\mathbf{s}_j)+\sum_{j=1}^{L}\gamma_2^j G_2(\mathbf{x},\mathbf{s}_j) \quad (20)$$

where the modified kernels $G_1(\mathbf{x},\mathbf{s})=\mathbf{i}\,[K_0(\lambda_1 r)-K_0(\lambda_2 r)]$ and $G_2(\mathbf{x},\mathbf{s})=K_0(\lambda_1 r)+K_0(\lambda_2 r)$ are real functions as shown in Appendix II.

To determine the unknowns, γ_1^j, γ_2^j, $\mathbf{s}_j$, boundary conditions in Eq. (11) should be imposed in suitable ways. For simplicity, the source points $\mathbf{s}_j$ are considered as *a priori* known, the boundary conditions are simply collocated at L boundary points $\mathbf{x}_i$. It results in a linear equations system as follows:

$$\bar{u}_1(\mathbf{x}_i)-B_1 u_p(\mathbf{x}_i)=\sum_{j=1}^{L}\gamma_1^j B_1 G_1(\mathbf{x}_i,\mathbf{s}_j)+\sum_{j=1}^{L}\gamma_2^j B_1 G_2(\mathbf{x}_i,\mathbf{s}_j)$$
$$\text{for} \quad i=1,2,\ldots,L \quad (21a)$$

$$\bar{u}_2(\mathbf{x}_i)-B_2 u_p(\mathbf{x}_i)=\sum_{j=1}^{L}\gamma_1^j B_2 G_1(\mathbf{x}_i,\mathbf{s}_j)+\sum_{j=1}^{L}\gamma_2^j B_2 G_2(\mathbf{x}_i,\mathbf{s}_j)$$
$$\text{for} \quad i=1,2,\ldots,L \quad (21b)$$

in which the B_1G_1, B_2G_1, B_1G_2, and B_2G_2 can be found by using Eq. (6). In other words, we require the partial derivatives $\frac{\partial G_1(r)}{\partial x_i}$, $\frac{\partial^2 G_1(r)}{\partial x_i \partial x_j}$, $\frac{\partial^3 G_1(r)}{\partial x_i \partial x_j \partial x_k}$, $\frac{\partial G_2(r)}{\partial x_i}$, $\frac{\partial^2 G_2(r)}{\partial x_i \partial x_j}$, and $\frac{\partial^3 G_2(r)}{\partial x_i \partial x_j \partial x_k}$ which are addressed in the appendix. In Eq. (21), there are $2L$ equations with $2L$ unknowns, γ_1^j, γ_2^j, and thus can be solved. The solvability of this linear equations system can be found in [16]. In this paper, we typically locate the boundary field points uniformly and place the source points stipulated out as depicted in Fig. 2 [24]. In which we define the parameter of source location b by

$$\mathbf{s}_i = \mathbf{c} + b(\mathbf{x}_i - \mathbf{c}) \quad (22)$$

where $\mathbf{c}$ is the geometric center.

Before closing the MFS-DRM formulations, it should be noticed that we can get the desired solution by using Eq. (8) if the complementary and particular solutions are both solved.

2.3 Particular Solutions

In this subsection, we address the particular solutions in Eq. (16). To be clearer, we are going to find particular solutions as follows:

$$D(\nabla^2\nabla^2+\lambda^4)\,F(r)=r^{2n}\ln r \quad (23a)$$

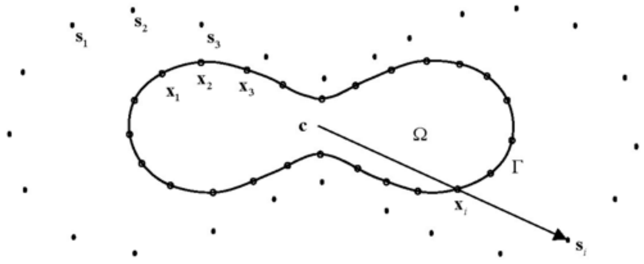

Fig. 2 Geometry configuration of the MFS

$$D(\nabla^2\nabla^2+\lambda^4)\,P(\mathbf{x})=x_1^s x_2^t \quad (23b)$$

In order to find the solutions of Eq. (23), we first introduce the difference trick [17]. If we have Ψ_1 and Ψ_2 such that

$$(\nabla^2-\lambda_1^2)\,\Psi_1=\varphi \quad (24a)$$

$$(\nabla^2-\lambda_2^2)\,\Psi_2=\varphi \quad (24b)$$

for some prescribed function φ. And, we are going to find Ψ such that

$$D(\nabla^2\nabla^2+\lambda^4)\,\Psi=\varphi \quad (25)$$

Compare Eqs. (24) and (25), we have

$$\Psi_1 = D(\nabla^2-\lambda_2^2)\,\Psi \quad (26a)$$

$$\Psi_2 = D(\nabla^2-\lambda_1^2)\,\Psi \quad (26b)$$

Subtract Eqs. (26) and suitably arrange terms, we can obtain the desired formula:

$$\Psi=\frac{\Psi_1-\Psi_2}{D(\lambda_1^2-\lambda_2^2)} \quad (27)$$

Now we are in a position to solve Eq. (23). Using the difference trick (Eq. (27)) and the particular solutions of splines and monomials for modified Helmholtz operator given in Cheng [18] and Golberg *et al.* [19] respectively, we are able to obtain:

$$F(r)=\frac{-4^n(n!)^2}{2D\mathbf{i}\,\lambda^{2n+4}}\left[K_0(\lambda e^{\mathbf{i}\frac{\pi}{4}}r)e^{-\mathbf{i}(n+1)\frac{\pi}{2}}-K_0(\lambda e^{-\mathbf{i}\frac{\pi}{4}}r)e^{\mathbf{i}(n+1)\frac{\pi}{2}}\right]$$
$$+\frac{4^n(n!)^2}{D}\sum_{m=1}^{n+1}\left\{\frac{r^{2m-2}\ln r}{4^{m-1}[(m-1)!]^2\lambda^{2n-2m+6}}\left(\sin(n-m+2)\frac{\pi}{2}\right)\right\}$$
$$+\frac{4^n(n!)^2}{D}\sum_{m=1}^{n}\left\{\frac{r^{2i-2}}{4^{m-1}[(m-1)!]^2\lambda^{2n-2m+6}}\left(\sum_{l=m}^{n}l^{-1}\right)\left(\sin(n-m+2)\frac{\pi}{2}\right)\right\}$$
$$(28a)$$

$$P(\mathbf{x})=\sum_{k=0}^{\left[\frac{s}{2}\right]}\sum_{l=0}^{\left[\frac{t}{2}\right]}\sin\frac{(k+l+1)\pi}{2}\,\frac{(k+l)!\,p!\,q!\,x_1^{s-2k}x_2^{t-2l}}{(\lambda)^{2k+2l+4}k!\,l!\,(s-2k)!\,(t-2l)!}$$
$$(28b)$$

This result has been checked by symbolic software MATHEMATICA.

Before closing this subsection, it should be mentioned that the RBF $f(r) = r^{2n} \ln r$, the corresponding particular solution and its partial derivatives may not be vanished when the Euclidean distance r approaches zero. Thus, the limit values are required in practical implementations, which are addressed in the Appendix I.

3. NUMERICAL RESULTS

In order to validate the proposed MFS-DRM formulations, we consider four numerical experiments as follows: a rectangle plate with clamped boundary condition, a rectangle plate with clamped and simply-supported boundary conditions, a rectangle plate with clamped and free boundary conditions, and a peanut-shaped plate. In these four numerical cases, we setup the exact solution as follows:

$$u(\mathbf{x}) = \sin\left(\frac{\pi x_1}{2}\right)\sin\left(\frac{\pi x_2}{2}\right) \tag{29}$$

which is the solution of

$$(\nabla^2\nabla^2 + \lambda^4)\, u = \frac{4\lambda^4 + \pi^4}{4}\sin\left(\frac{\pi x_1}{2}\right)\sin\left(\frac{\pi x_2}{2}\right) \tag{30}$$

In all the numerical experiments, boundary conditions are set up according to these exact solutions. Also, $D = 1$ and $v = 0.33$ are assumed. After the validations of MFS-DRM formulations, we apply it to a benchmarked problem of a circular plate under uniform loading.

In addition, we define the root-mean-square error as

$$\sqrt{\frac{\sum_{i=1}^{\bar{N}} (u_{\text{numerical}}(\mathbf{x}_i) - u_{\text{exact}}(\mathbf{x}_i))^2}{\bar{N}}} \tag{31}$$

where $u_{\text{numerical}}(\mathbf{x}_i)$ is the numerical solutions obtained by the MFS-DRM equation (8) at $\mathbf{x}_i$, $u_{\text{exact}}(\mathbf{x}_i)$ is the corresponding exact solution, and $\bar{N}$ is the number of total nodes considered.

Case I: A rectangle Plate with Clamped Boundary Condition

We consider a square plate of size 2×2 suggested to clamped boundary conditions. Figure 3 gives the condition numbers and root-mean-square errors versus the parameter of source location. It is found that farther sources or larger ranks give worse conditioning but better accuracies. In the above descriptions, the rank is defined by the rank of the matrix resulted from Eq. (21). This situation can be predicted by the general theory of MFS proposed in [24]. The best root-mean- square errors, $10^{-6} \sim 10^{-9}$, are achieved when $b = 2 \sim 4$. It is interesting to find that the accuracies do not get worse for $b > 2 \sim 4$.

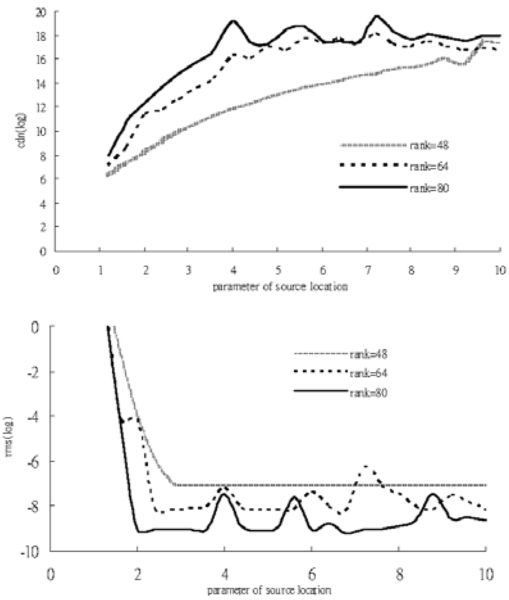

Fig. 3 The condition numbers (up) and errors (down) and of case I

Case II: A Rectangle Plate with Clamped and Simply-Supported Boundary Conditions

Then, we consider the same problem by imposing simply-supported boundary condition on one edge. Figure 4 describes the condition numbers and root-mean-square errors versus the parameter of source location. Similarly, better accuracies and worse conditioning are found for farther source or larger rank. These phenomena are similar to the previous case and the theoretical prediction [24]. The best root-mean-square errors are also in the range $10^{-6} \sim 10^{-9}$ when $b = 2 \sim 4$. Also, the errors are hold for $b > 2 \sim 4$. From these results, it is also demonstrated that the MFS-DRM is able to solve the plate loading problems with simply-supported boundary condition accurately and stably.

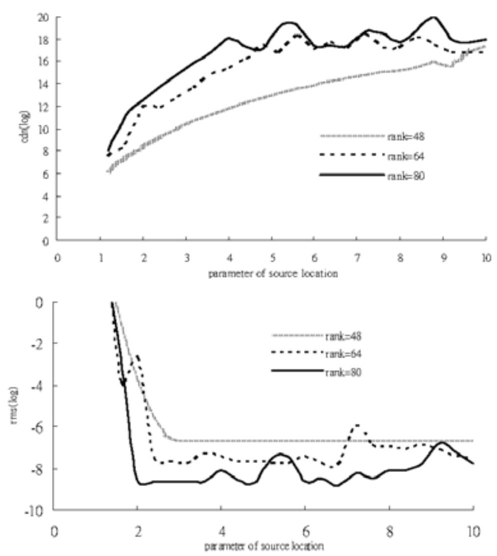

Fig. 4 The condition numbers (up) and errors (down) and of case II

Case III: A Rectangle Plate with Clamped and Free Boundary Conditions

Similarly, we replace the simply-supported boundary condition of the previous case by free boundary condition. Figure 5 gives the condition numbers and root-mean-square errors for the problem. It is observed the best accuracies $10^{-5} \sim 10^{-8}$ are achieved for $b = 2 \sim 4$, which are also of great accuracies although slightly worse than the previous two cases. Also, better accuracies are found for larger rank. On the other hand, in this case the accuracies become worse when b is larger than the best value. The reason is not clear. Overall, the MFS-DRM can also solve plate loading problems with free boundary condition accurately.

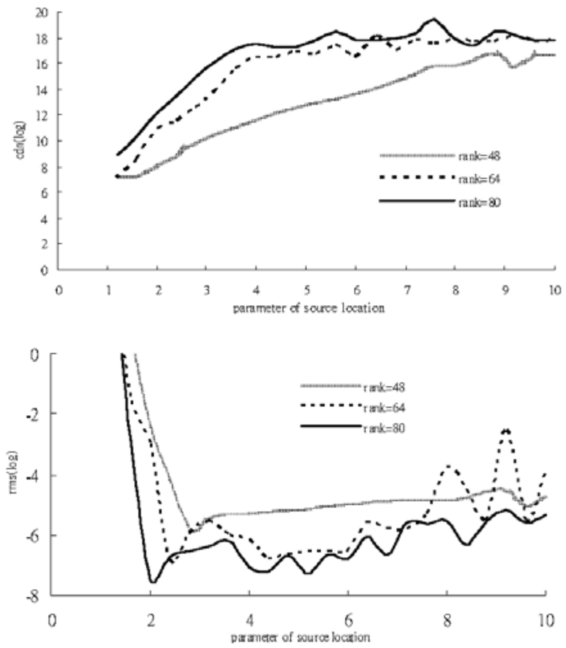

Fig. 5 The condition numbers (up) and errors (down) and of case III

Case IV: A Peanut-Shaped Plate

In order to demonstrate the flexibility of the proposed numerical method to treat irregular domains, a peanut-shaped plate, depicted in Figs. 1 and 2, subjected to clamped boundary condition. The exact solution is the same as the previous cases. Figure 6 gives the condition numbers and root-mean-square errors for the problem. Although the accuracies are not perfect as the previous three cases, the errors are general good in the range $10^{-4} \sim 10^{-6}$.

Case V: Circular Plate under Uniform Loading

After validating the MFS-DRM formulations, we consider the benchmarked problem of a circular plate under uniform loading. The analytical solution of the problem is

$$u(r) = \frac{q_0}{D\lambda^4} + \bar{a}J_0(\lambda_1 r) + \bar{b}J_0(\lambda_2 r) \qquad (32)$$

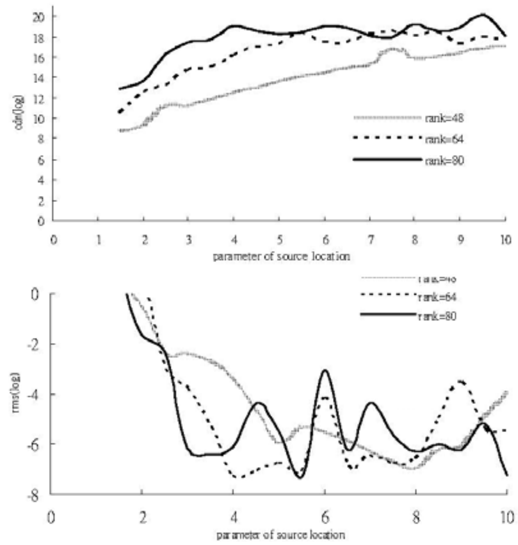

Fig. 6 The condition numbers (up) and errors (down) and of case IV

with

$$\begin{cases} \bar{a} = \dfrac{q_0 \lambda_2 J_1(\lambda_2 R)}{D\lambda^4[\lambda_1 J_0(\lambda_2 R) J_1(\lambda_1 R) - \lambda_2 J_0(\lambda_1 R) J_1(\lambda_2 R)]} \\ \bar{b} = \dfrac{-q_0 \lambda_1 J_1(\lambda_1 R)}{D\lambda^4[\lambda_1 J_0(\lambda_2 R) J_1(\lambda_1 R) - \lambda_2 J_0(\lambda_1 R) J_1(\lambda_2 R)]} \end{cases} \qquad (33)$$

where q_0 is the density of uniform loading and R is the radius of the plate. Figure 7 depicts the condition numbers and root-mean-square errors for the problem. The errors are general good in the range $10^{-11} \sim 10^{-13}$, which is much better than the previous cases since the particular solution is analytical.

4. CONCLUSIONS

In this paper, the combination of the method of fundamental solutions (MFS) and the dual reciprocity method (DRM) is proposed as a meshless numerical method to solve thin plates resting on Winkler foundations under arbitrary loadings. In the DRM, the arbitrary distributed loadings are approximated by the augmented polyharmonic splines. Then, the nonhomogeneous solutions are able to be represented by a series of the analytical particular solutions of splines and monomials. The complementary solutions are then solved by the MFS. In addition, the boundary conditions of lateral displacement, slope, normal moment, and effective shear force are all given explicitly for the particular solutions of DRM as well as the kernels of MFS.

To validate the proposed numerical method, three numerical experiments of clamped, clamped and simply-supported, and clamped and free boundary conditions are carried out. Then, the method is applied to a problem of peanut-shaped domain to demonstrate the flexibility of the proposed numerical method to treat irregular domains. Also, the benchmarked problem of

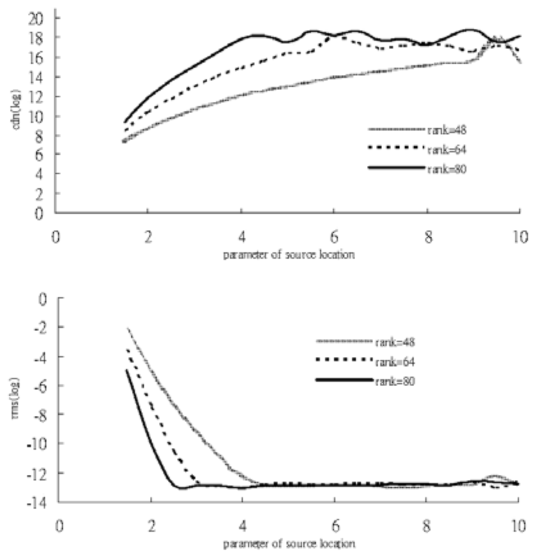

Fig. 7 The condition numbers (up) and errors (down) and of case V

a circular plate under uniform loading is considered. From these results, it is convienced that the MFS-DRM is a suitable meshless numerical method to solve Kirchhoff plates resting on Winkler foundations under arbitrary loadings without integrations and singularities.

ACKNOWLEDGEMENTS

I appreciate an anonymous reviewer provided the proof in Appendix II. Also, the National Science Council of Taiwan is gratefully acknowledged for providing financial support to carry out the present work under the grant No. NSC95-2221-E-464-002 and NSC96-2221-E-464-001.

APPENDIX I

PARTIAL DERIVATIVES OF PARTICULAR SOLUTIONS AND THEIR LIMITS FOR $R \to 0$

The partial derivatives of the particular solutions of DRM and the kernels of MFS are given as follows:

$$\frac{\partial F(r)}{\partial x_i} = x_i \frac{F'}{r} \tag{A1}$$

$$\frac{\partial^2 F(r)}{\partial x_i \partial x_j} = \delta_{ij}\frac{F'}{r} + x_i x_j \frac{rF'' - F'}{r^3} \tag{A2}$$

$$\frac{\partial^3 F(r)}{\partial x_i \partial x_j \partial x_k} = (\delta_{ij}x_k + \delta_{ik}x_j + \delta_{jk}x_i)\frac{rF'' - F'}{r^3} + x_i x_j x_k \frac{r^2 F''' - 3rF'' + 3F'}{r^5} \tag{A3}$$

with

$$\frac{F'}{r} = \frac{4^n (n!)^2}{2D\mathbf{i}\,\lambda^{2n+4}}\left\{\frac{\lambda e^{-\mathbf{i}(2n+1)\frac{\pi}{4}} K_1(\lambda e^{\mathbf{i}\frac{\pi}{4}} r) - \lambda e^{\mathbf{i}(2n+1)\frac{\pi}{4}} K_1(\lambda e^{-\mathbf{i}\frac{\pi}{4}} r)}{r}\right\} + \frac{4^n (n!)^2}{D}\sum_{m=1}^{n+1}\left\{\frac{r^{2m-4}[1+2(m-1)\ln r]}{4^{m-1}[(m-1)!]^2 \lambda^{2n-2m+6}}\sin(n-m+2)\frac{\pi}{2}\right\}$$
$$+\frac{4^n (n!)^2}{D}\sum_{m=1}^{n}\left\{\frac{2(m-1)r^{2m-4}}{4^{m-1}[(m-1)!]^2 \lambda^{2n-2m+6}}\left(\sum_{l=m}^{n} l^{-1}\right)(\sin(n-m+2)\frac{\pi}{2}\right\} \tag{A4}$$

$$\frac{rF'' - F'}{r^3} = \frac{-4^n (n!)^2}{2D\mathbf{i}\,\lambda^{2n+4}}\left[\frac{\lambda^2 e^{-\mathbf{i}\frac{n\pi}{2}} K_2(\lambda e^{\mathbf{i}\frac{\pi}{4}} r) - \lambda^2 e^{\mathbf{i}\frac{n\pi}{2}} K_2(\lambda e^{-\mathbf{i}\frac{\pi}{4}} r)}{r^2}\right] + \frac{4^n (n!)^2}{D}\sum_{m=1}^{n+1}\left\{\frac{r^{2m-6}[(4m-6)+4(m-1)(m-2)\ln r]}{4^{m-1}[(m-1)!]^2 \lambda^{2n-2m+6}}\sin(n-m+2)\frac{\pi}{2}\right\}$$
$$+\frac{4^n (n!)^2}{D}\sum_{m=1}^{n}\left\{\frac{4(m-1)(m-2)r^{2m-6}}{4^{m-1}[(m-1)!]^2 \lambda^{2n-2m+6}}\left(\sum_{l=m}^{n} l^{-1}\right)(\sin(n-m+2)\frac{\pi}{2}\right\} \tag{A5}$$

$$\frac{r^2 F''' - 3rF'' + 3F'}{r^5} = \frac{4^n (n!)^2}{2D\mathbf{i}\,\lambda^{2n+4}}\left[\frac{\lambda^3 e^{-\mathbf{i}(2n-1)\frac{\pi}{4}} K_3(\lambda e^{\mathbf{i}\frac{\pi}{4}} r) - \lambda^3 e^{\mathbf{i}(2n-1)\frac{\pi}{4}} K_3(\lambda e^{-\mathbf{i}\frac{\pi}{4}} r)}{r^3}\right]$$
$$+\frac{4^n (n!)^2}{D}\sum_{m=1}^{n+1}\left\{\frac{4r^{2m-8}[11+3m(m-4)+2(m-1)(m-2)(m-3)\ln r]}{4^{m-1}[(m-1)!]^2 \lambda^{2n-2m+6}}\sin(n-m+2)\frac{\pi}{2}\right\}$$
$$+\frac{4^n (n!)^2}{D}\sum_{m=1}^{n}\left\{\frac{8(m-1)(m-2)(m-3)r^{2m-8}}{4^{m-1}[(m-1)!]^2 \lambda^{2n-2m+6}}\left(\sum_{l=m}^{n} l^{-1}\right)\sin(n-m+2)\frac{\pi}{2}\right\} \tag{A6}$$

and,

$$\frac{\partial G_1}{\partial x_i} = \frac{\mathbf{i}\, x_i[-\lambda e^{\mathbf{i}\frac{\pi}{4}} K_1(\lambda e^{\mathbf{i}\frac{\pi}{4}} r) + \lambda e^{-\mathbf{i}\frac{\pi}{4}} K_1(\lambda e^{-\mathbf{i}\frac{\pi}{4}} r)]}{r} \tag{A7}$$

$$\frac{\partial^2 G_1}{\partial x_i \partial x_j} = \frac{\mathbf{i}\, x_i x_j [\lambda^2 e^{\mathbf{i}\frac{\pi}{2}} K_2(\lambda e^{\mathbf{i}\frac{\pi}{4}} r) - \lambda^2 e^{-\mathbf{i}\frac{\pi}{2}} K_2(\lambda e^{-\mathbf{i}\frac{\pi}{4}} r)]}{r^2} + \frac{\mathbf{i}\, \delta_{ij} [-\lambda e^{\mathbf{i}\frac{\pi}{4}} K_1(\lambda e^{\mathbf{i}\frac{\pi}{4}} r) + \lambda e^{-\mathbf{i}\frac{\pi}{4}} K_1(\lambda e^{-\mathbf{i}\frac{\pi}{4}} r)]}{r} \quad \text{(A8)}$$

$$\frac{\partial^3 G_1}{\partial x_i \partial x_j \partial x_k} = \frac{\mathbf{i}\, x_i x_j x_k [-\lambda^3 e^{\mathbf{i}\frac{3\pi}{4}} K_3(\lambda e^{\mathbf{i}\frac{\pi}{4}} r) + \lambda^3 e^{-\mathbf{i}\frac{3\pi}{4}} K_3(\lambda e^{-\mathbf{i}\frac{\pi}{4}} r)]}{r^3} + \frac{\mathbf{i}\, (\delta_{ij} x_k + \delta_{jk} x_i + \delta_{ki} x_j)[\lambda^2 e^{\mathbf{i}\frac{\pi}{2}} K_2(\lambda e^{\mathbf{i}\frac{\pi}{4}} r) - \lambda^2 e^{-\mathbf{i}\frac{\pi}{2}} K_2(\lambda e^{-\mathbf{i}\frac{\pi}{4}} r)]}{r^2} \quad \text{(A9)}$$

$$\frac{\partial G_2}{\partial x_i} = \frac{-x_i [\lambda e^{\mathbf{i}\frac{\pi}{4}} K_1(\lambda e^{\mathbf{i}\frac{\pi}{4}} r) + \lambda e^{-\mathbf{i}\frac{\pi}{4}} K_1(\lambda e^{-\mathbf{i}\frac{\pi}{4}} r)]}{r} \quad \text{(A10)}$$

$$\frac{\partial^2 G_2}{\partial x_i \partial x_j} = \frac{x_i x_j [\lambda^2 e^{\mathbf{i}\frac{\pi}{2}} K_2(\lambda e^{\mathbf{i}\frac{\pi}{4}} r) + \lambda^2 e^{-\mathbf{i}\frac{\pi}{2}} K_2(\lambda e^{-\mathbf{i}\frac{\pi}{4}} r)]}{r^2} + \frac{-\delta_{ij} [\lambda e^{\mathbf{i}\frac{\pi}{4}} K_1(\lambda e^{\mathbf{i}\frac{\pi}{4}} r) + \lambda e^{-\mathbf{i}\frac{\pi}{4}} K_1(\lambda e^{-\mathbf{i}\frac{\pi}{4}} r)]}{r} \quad \text{(A11)}$$

$$\frac{\partial^3 G_2}{\partial x_i \partial x_j \partial x_k} = \frac{-x_i x_j x_k [\lambda^3 e^{\mathbf{i}\frac{3\pi}{4}} K_3(\lambda e^{\mathbf{i}\frac{\pi}{4}} r) + \lambda^3 e^{-\mathbf{i}\frac{3\pi}{4}} K_3(\lambda e^{-\mathbf{i}\frac{\pi}{4}} r)]}{r^3} + \frac{(\delta_{ij} x_k + \delta_{jk} x_i + \delta_{ki} x_j)[\lambda^2 e^{\mathbf{i}\frac{\pi}{2}} K_2(\lambda e^{\mathbf{i}\frac{\pi}{4}} r) + \lambda^2 e^{-\mathbf{i}\frac{\pi}{2}} K_2(\lambda e^{-\mathbf{i}\frac{\pi}{4}} r)]}{r^2} \quad \text{(A12)}$$

The partial derivatives of $P(\mathbf{x})$ are straightforward and are neglected here. In addition, we have the following limit values as r approaches zero for $f(r) = r^{2n} \ln r$, the corresponding particular solution and its partial derivatives:

$$\lim_{r \to 0} f = 0 \quad \text{(A13)}$$

$$\lim_{r \to 0} F = \frac{4^n (n!)^2 \left\{ \frac{\pi}{4} \cos \frac{(n+1)\pi}{2} + \left(\ln \frac{2}{r_0} - \Upsilon + \sum_{l=1}^{n} l^{-1} \right) \sin \frac{(n+1)\pi}{2} \right\}}{D\, r_0^{2n+4}} \quad \text{(A14)}$$

$$\lim_{r \to 0} \frac{F'}{r} = \frac{4^n (n!)^2 \left\{ \frac{\pi}{4} \cos \frac{n\pi}{2} + \left(\ln \frac{2}{r_0} - \Upsilon + \sum_{l=1}^{n} l^{-1} \right) \sin \frac{n\pi}{2} \right\}}{2D\, r_0^{2n+2}} \quad \text{(A15)}$$

$$\lim_{r \to 0} \frac{rF'' - F'}{r^3} = \frac{4^n (n!)^2 \left\{ \frac{\pi}{4} \cos \frac{(n-1)\pi}{2} + \left(\ln \frac{2}{r_0} - \Upsilon + \sum_{l=1}^{\mathrm{Max}\{2,n\}} l^{-1} \right) \sin \frac{(n-1)\pi}{2} \right\}}{8D\, r_0^{2n}} \quad \text{(A16)}$$

$$\lim_{r \to 0} \frac{r^2 F''' - 3rF'' + 3F'}{r^5} = \frac{4^n (n!)^2 \left\{ \frac{\pi}{4} \cos \frac{(n-2)\pi}{2} + \left(\ln \frac{2}{r_0} - \Upsilon + \sum_{l=1}^{\mathrm{Max}\{3,n\}} l^{-1} \right) \sin \frac{(n-2)\pi}{2} \right\}}{48D\, r_0^{2n-2}} \quad \text{(A17)}$$

APPENDIX II

THE REAL KERNELS

In order to show the kernels in Eq. (20) are real, we can begin with the following expression for the zero order modified Bessel function of second kink defined by Tikhonov and Samarskii [25]:

$$K_0(x) = \frac{1}{2} \int_{-\infty}^{\infty} e^{-x \cos \eta} d\eta \quad \text{(A18)}$$

By using the definition of

$\lambda_1 = \lambda e^{\mathbf{i}\frac{\pi}{4}} = \lambda \left(\cos \frac{\pi}{4} + \mathbf{i} \sin \frac{\pi}{4} \right)$ we have

$$\begin{aligned} K_0(\lambda_1 r) &= \frac{1}{2} \int_{-\infty}^{\infty} e^{-\lambda r (\cos \frac{\pi}{4} + \mathbf{i} \sin \frac{\pi}{4}) \cos \eta} d\eta \\ &= \frac{1}{2} \int_{-\infty}^{\infty} e^{-\lambda r \cos \frac{\pi}{4} \cos \eta} \cos \left(\lambda r \sin \frac{\pi}{4} \cos \eta \right) d\eta \\ &\quad - \frac{\mathbf{i}}{2} \int_{-\infty}^{\infty} e^{-\lambda r \cos \frac{\pi}{4} \cos \eta} \sin \left(\lambda r \sin \frac{\pi}{4} \cos \eta \right) d\eta \end{aligned} \quad \text{(A19)}$$

Similarly, we have the following equation by utilizing

$$\lambda_2 = \lambda e^{-\mathbf{i}\frac{\pi}{4}} = \lambda\left(\cos\frac{\pi}{4} - \mathbf{i}\sin\frac{\pi}{4}\right)$$

$$K_0(\lambda_2 r) = \frac{1}{2}\int_{-\infty}^{\infty} e^{-\lambda r\cos\frac{\pi}{4}\cos\eta}\cos\left(\lambda r\sin\frac{\pi}{4}\cos\eta\right)d\eta + \frac{\mathbf{i}}{2}\int_{-\infty}^{\infty} e^{-\lambda r\cos\frac{\pi}{4}\cos\eta}\sin\left(\lambda r\sin\frac{\pi}{4}\cos\eta\right)d\eta \quad \text{(A20)}$$

Eqs. (A19) and (A20) are sufficient to demonstrate the kernels $G_1(\mathbf{x}, \mathbf{s})$ and $G_2(\mathbf{x}, \mathbf{s})$ in Eq. (20) are real functions.

REFERENCES

1. Kansa, E. J., "Multiquadrics—A Scattered Data Approximation Scheme with Applications to Computational Fluid Dynamics—II. Solutions to Parabolic, Hyperbolic and Elliptic Partial Differential Equations," *Computers and Mathematics with Applications*, 19, pp. 147–161 (1990).
2. Kupradze, V. D. and Aleksidze, M. A., "The Method of Functional Equations for the Approximate Solution of Certain Boundary Value Problem," *USSR Computational Mathematics and Mathematical Physics*, 4, pp. 82–126 (1964).
3. Young, D. L., Chen, K. H. and Lee, C. W., "Novel Meshless Method for Solving the Potential Problems with Arbitrary Domain," *Journal of Computational Physics*, 209, pp. 290–321 (2005).
4. Young, D. L., Chen, K. H., Chen, J. T. and Kao, J. H., "A Modified Method of Fundamental Solutions with Source on the Boundary for Solving Laplace Equation with Circular and Arbitrary Domains," *CMES: Computer Modeling in Engineering and Sciences*, 19, pp. 197–221 (2007).
5. Chen, K. H., Chen, J. T. and Kao, J. H., "Regularized Meshless Method for Solving Acoustic Eigenproblem with Multiply Connected Domain," *Computer Modeling in Engineering Science*, 16, pp. 27–39 (2006).
6. Chen, K. H., Kao, J. H., Chen, J. T., Young, D. L. and Lu, M. C., "Regularized Meshless Method for Multiply-Connected—Domain Laplace Problems," *Engineering Analysis with Boundary Elements*, 30, pp. 882–896 (2006).
7. Fairweather, G. and Karageorghis, A., "The Method of Fundamental Solutions for Elliptic Boundary Value Problems," *Advances in Computational Mathematics*, 9, pp. 69–95 (1998).
8. Fairweather, G., Karageorghis, A. and Martin, P. A., "The Method of Fundamental Solutions for Scattering and Radiation Problems," *Engineering Analysis with Boundary Elements*, 27, pp. 759–769 (2003).
9. Li, J., Hon, Y. C. and Chen, C. S., "Numerical Comparisons of Two Meshless Methods Using Radial Basis Function," *Engineering Analysis with Boundary Elements*, 26, pp. 205–225 (2002).
10. Tsai, C. C., Young, D. L. and Fan, C. M., "Method of Fundamental Solutions for Plate Vibrations in Multiply Connected Domains," *Journal of Mechanics*, 22, pp. 235–245 (2006).
11. Chen, J. T., Chen, I. L. and Lee, Y. T., "Eigensolutions of Multiply-Connected Membranes Using Method of Fundamental Solution," *Engineering Analysis with Boundary Elements*, 29, pp. 166–174 (2005).
12. Nardini, D. and Brebbia, C. A., "A New Approach to Free Vibration Analysis Using Boundary Elements," Brebbia, C. A., Ed., *Boundary Element Methods in Engineering*, pp. 312–326 (1982).
13. Golberg, M. A., "The Method of Fundamental Solutions for Poisson's Equation," *Engineering Analysis with Boundary Elements*, 16, pp. 205–213 (1995).
14. Golberg, M. A. and Chen, C. S., "The Method of Fundamental Solutions for Potential, Helmholtz and Diffusion Problems," Golberg, M. A., Ed., *Boundary Integral Methods: Numerical and Mathematical Aspects*, pp. 103–176 (1998).
15. Duchon, J., "Splines Minimizing Rotation Invariant Semi-Norms in Sobolev Spaces," Schempp, W., and Zeller, K., Eds., *Constructive Theory of Functions of Several Variables*, pp. 85–100 (1977).
16. Bogomolny, A., "Fundamental Solutions Method for Elliptic Boundary Value Problems," *SIAM Journal on Numerical Analysis*, 22, pp. 644–669 (1985).
17. Banerjee, P. K., *The Boundary Element Methods in Engineering*, McGraw-Hill, London (1994).
18. Cheng, A. H.-D., "Particular Solutions of Laplacian, Helmholtz-Type, and Polyharmonic Operators Involving Higher Order Radial Basis Functions," *Engineering Analysis with Boundary Elements*, 24, pp. 531–538 (2000).
19. Golberg, M. A., Muleshkov, A. S., Chen, C. S. and Cheng, A. H.-D., "Polynomial Particular Solutions for Some Partial Differential Operators," *Numerical Methods for Partial Differential Equations*, 19, pp. 112–133 (2003).
20. Reutskiy, S. Y. and Chen, C. S., "Approximation of Multivariate Functions and Evaluation of Particular Solutions Using Chebyshev Polynomial and Trigonometric Basis Functions," *International Journal for Numerical Methods in Engineering*, 67, pp. 1811–1829 (2006).
21. Muleshkov, A. S. and Golberg, M. A., "Particular Solutions of the Multi-Helmholtz-Type Equation," *Engineering Analysis with Boundary Elements*, 31, pp. 624–630 (2007)
22. Costa, J. A. and Brebbia, C. A., "The Boundary Element Method Applied to Plates on Elastic Foundations," *Engineering Analysis with Boundary Elements*, 2, pp. 174–182 (1995).
23. Costa, J. A. and Brebbia, C. A., "On the Reduction of Domain Integrals to the Boundary for the BEM Formulation of Plates on Elastic Foundations," *Engineering Analysis with Boundary Elements*, 3, pp. 123–126 (1986).
24. Tsai, C. C., Lin, Y. C., Young, D. L. and Atluri, S. N., "Investigations on the Accuracy and Condition Number for the Method of Fundamental Solutions," *CMES: Computer Modeling in Engineering and Sciences*, 16, pp. 103–114 (2006).
25. Tikhonov, A. N. and Samarskii, A. A., *Equations of Mathematical Physics*, The MacMillan Company, New York (1973).

(Manuscript received May 21, 2007,
accepted for publication January 8, 2008.)